Received June 19, 2017, accepted July 9, 2017, date of publication July 31, 2017, date of current version August 22, 2017.

Digital Object Identifier 10.1109/ACCESS.2017.2731779

A Novel Control Approach for a Thrust Vector System With an Electromechanical Actuator

BING YU AND WENJUN SHU

Jiangsu Province Key Laboratory of Aerospace Power Systems, College of Energy and Power Engineering, Nanjing University of Aeronautics and Astronautics, Nanjing 210016, China

Corresponding author: Bing Yu (yb203@nuaa.edu.cn)

This work was supported in part by the Natural Science Foundation of China under Grant 51406083, in part by the Fundamental Research Funds for the Central Universities under Grant NJ20160037, and in part by the Natural Science Foundation of Jiangsu Province under Grant BK20140820.

ABSTRACT A novel control scheme for a thrust vector system with an electromechanical actuator is proposed. The proposed method merges the idea exploited in sliding mode control (SMC) with proportion–integration–differentiation (PID) control, which brings advantages in terms of strong robustness and good position tracking performance, while the chattering of the control signal produced by the SMC is small. A model for a typical thrust vector system with an electromechanical actuator is established and analyzed. To evaluate the performance of the proposed approach, the traditional PID controller mixed with bang-bang control and the proposed compound control law is applied to the two-channel model of the thrust vector system with an electromechanical actuator. Various simulation examples are provided to show that this compound control law has stronger robustness to the model parameter uncertainty and better position tracking performance. In addition, the chattering is slight.

INDEX TERMS Electromechanical actuator (EMA), sliding mode control (SMC), thrust vector system (TVC).

NOMENCLATURE

$a_{1,2,3}$, b_1	Coefficients of the nominal dynamic model.
$\widetilde{a}_{1,2,3}$, $\widetilde{b}_1$	Coefficients of the actual dynamic model.
B	Pitch of the ball-screw.
B_a	Damping coefficient of brushless direct current motor.
B_n	Coefficient of viscous damping of the load.
D	Moment arm of the actuator about the load pivot.
d	Interference and modeling uncertainty.
e_m	Tracking error of the slide model controller.
I	Motor armature current.
i_g	Deceleration ratio of the gears.
J_a	Moment of inertia of brushless direct current motor.
J_n	Inertia of the load on the actuator swing-plane.
k_i	Compensation coefficient of the input in the ith actuator (i=1,2).
K_l	Stiffness of the drive rod.
K_m	Motor back electromotive force constant.
K_n	Coefficient of the elastic torque of the load.
K_T	Torque constant of brushless direct current motor.
L	Motor armature inductance.
L_b	Pitch of the ball-screw.
q_i	Pitch and yaw angles of the nozzle (i=1,2).
R	Motor armature resistance.
T_{ib}	Euler angle transformation matrix (i=1,2).
T_L	Load into brushless direct current motor.
T_n	Ratio of motor rotation to drive rod translation.
u	Applied average motor armature voltage of the actuator.
X_{ij}	Four position vectors of the actuators to calculate transformation functions ($i = 0, 1; j = 1, 2$).
y_a	Linear displacement output of the actuator at the input end of the ball-screw.
y_d	Desired linear displacement of the actuator.
y_n	Linear displacement output of the actuator at the load end.
α	Rotating angle of the motor rotor.
β	Swaying angle of the motor.
ϵ_i	Solved compensation input of the ith actuator (i=1,2).

$\xi_{p,n}$ Damping coefficient of the peak filter and the notch filter.
λ_i Switching function parameters of sliding mode controller (i=1,2).
σ_i Two parameters of the sliding surface (i=1,2).

I. INTRODUCTION

With the development of some special aircraft, such as rockets and missiles, the demand for high maneuvering flight continues to increase, and thrust vector control (TVC) has become particularly important [1], [2]. Thrust vector control employs nozzle deflection to produce a propulsive component to increase the incidence angle and thus maneuvers the vehicle through the ensuing aerodynamic forces. And A common feature is the deflection of the propulsive vector from the vehicle centerline in order to produce a moment about the center of the mass of the vehicle [3], [4]. TVC uses the manipulation of the engine thrust direction to achieve the attitude adjustment of a vehicle and has the advantages of a small axial thrust loss, a fast dynamic response, and a large control function [5].

The use of electromechanical actuators (EMAs) is becoming increasingly popular in the aerospace industry because of their attractive characteristics such as simplicity, reliability, low cost, good dynamic characteristics, momentary overdrive capability and easy control. EMAs are being used in many situations where hydraulic systems have been employed almost exclusively in the past with their disadvantages such as poor maintenance, sensitivity to oil temperature, and leakage problems [6]–[9]. For these reasons, the thrust vector control with an electromechanical actuator (TVC-EMA) system has attracted much attention.

For the controller design, the model is subject to uncertainties from several sources: perpetual parametric variations caused by temperature changes, aging, un-modeled dynamics, load changes, and asymmetric behavior, as well as large combustion transients at engine startup and shutdown [10]. Therefore, it is desirable to develop an EMA controller that can provide strong robustness. Sliding mode control (SMC) is an effective control method with strong robustness [11]–[14]. For over fifty years, SMC has been widely studied and extensively employed in many applications [15]–[18]. One of the most intriguing aspects of sliding mode is the discontinuous nature of the control action whose primary function of each of the feedback channels is to switch between two distinctively different system structures such that a new type of system motion, called sliding mode. This peculiar system characteristic is claimed to result in superb system performance which includes insensitivity to parameter variations, and complete rejection of disturbances. And the disadvantage of this method is that when the state trajectory reaches the sliding surface, it is difficult to strictly slide along the sliding surface toward the equilibrium point, but on both sides of the sliding surface through the back and forth, resulting in vibration [19].

Ílyas Eker proposed a second-order sliding mode control with a proportion-integration (PI) sliding surface for an electromechanical plant, and experimental results demonstrated that the 2-SMC system had better tracking specifications than PID control [20]. Lu *et al*. adopted $H\infty$ control and μ synthesis theory for TVC to suppress the model perturbation in the large inertial tracking problem [21]. Li *et al*. proposed a very efficient controller to supplement this work, designing a compound control law composed of a PID controller and bang-bang control [7]. Wang *et al*. proposed a robust controller through the sliding-mode variable structure approach for one channel in TVC-EMA [22].

However, some problems have been neglected in previous studies. For example, the nozzle pivots about a gimbal jointly driven by two actuators that are mounted 90° apart around the circumference of the engine, which can make the nozzle realize coordinated motion in the pitch and yaw directions [7], [22], but neither the model perturbation nor the disturbance force were studied with the two-channel coupling problem, that is the nozzle motion has strong coupling between the pitching and yawing directions. A controller based on SMC was also studied with the coupling problem to solve the coordinated motion of two actuators. The purpose of this paper is to present a novel control method to improve the overall performance of the TVC-EMA system, including stability, precision, rapidity and robustness, when the nozzle is driven by two actuators. One of main contributions of this paper is its consideration of this structure with nominal model for this kind of application.

The remainder of this paper is organized as follows. In Section II, the considered thrust vector control system with an electromechanical actuator (TVC-EMA system) is illustrated. Section III introduces the control block diagram and the compound control law. Section IV presents the nominal model of the TVC-EMA system based on resonance suppression, and Section V designs the SMC controller and analyzes its stability. A simulation of the TVC-EMA system is performed and the results are analyzed in Section VI, and Section VII draws the conclusions of this paper.

II. DESCRIPTION OF THE TVC-EMA SYSTEM

According to the dynamic performance indexes for the single-channel actuator in [21] and the coupled motion of the nozzle between the pitch and yaw channels in [7], the detailed demands of the dynamic performance in the step response of the pitch and yaw angles are the following: settling time is less than 0.2 seconds, the steady-state error is smaller than 1%, and the overshoot should be limited to less than 1%.

The typical configuration of TVC-EMA in an aircraft is shown in Fig. 1. The nozzle pivots about a gimbal jointly driven by two actuators that enables the nozzle to realize coordinated motion in the pitch and yaw directions.

To carry out a control study of the EMA system, the mathematical modeling should first be investigated. Many modeling studies on the EMA system have previously been reported. Sang Hwa Kim and Min Jea Tahk presented a

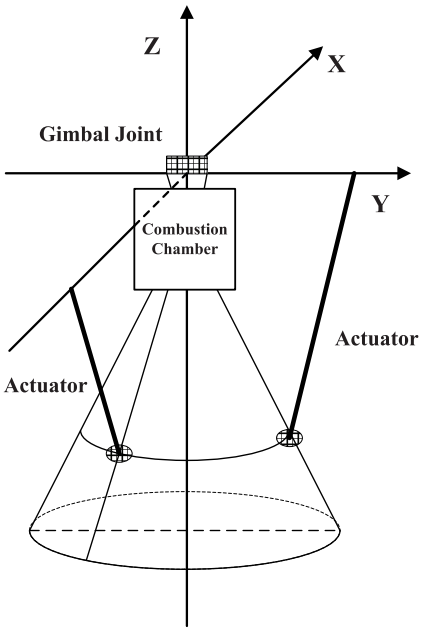

FIGURE 1. Configuration of the thrust vector control system with an electromechanical actuator.

method for the modeling of the dynamic stiffness of an electromechanical actuator [23] and proposed an approach for handling large static stiffness values of the EMA components. Schinstock *et al*. presented a linearized model of TVC-EMA for rocket engines along with effective methods of estimating the model parameters [24]. Rafik Salloum *et al*. used experimental identification and structured and unstructured uncertainty modeling for designing an EMA system with a harmonic drive, and a robust PID controller based on the Kharitonov method was designed [25]. The modeling is not the focus in this paper; rather, we have proposed a novel control scheme and verified it. A typical EMA system without a controller mainly comprises a brushless direct current motor (BLDCM), a transmission mechanism including gears and a ball screw, and a displacement sensor. The generic BLDCM voltage equations can be written as [23]

$$u = K_m\dot{\alpha} + RI + L\dot{I} \tag{1}$$

The relation between the electromagnetic torque (T_L) and the mechanical angular velocity ($\dot{\alpha}$) of the motor can be written as

$$K_T I = T_L + J_a\ddot{\alpha} + B_a\dot{\alpha} \tag{2}$$

The transmission mechanism transforms angular displacement (α) to linear displacement (y_a), and its function can be described as

$$y_a = \frac{\alpha L_b}{2\pi N_g} \tag{3}$$

The mathematical model of the nozzle can be written as

$$T_n = DK_l(y_a - y_n) = J_n\ddot{\beta} + B_n\dot{\beta} + K_n\beta \tag{4}$$

The relation between the load torque (T_n) and the electromagnetic torque (T_L) can be written as

$$T_L = \frac{B}{2\pi i_g D}\cdot\frac{T_n}{\eta_a} \tag{5}$$

Because the angles in the TVC-EMA system are small, usually no greater than 10°, the linear displacement of the actuator by the angle of the nozzle can be expressed as

$$y_n = D\beta \tag{6}$$

The transmission structure of TVC-EMA in one channel is shown in Fig. 2.

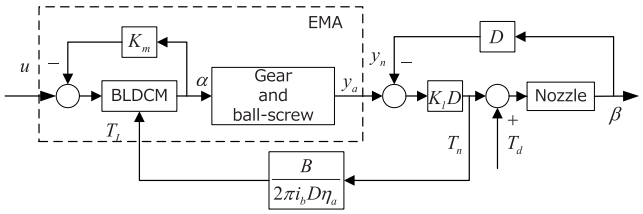

FIGURE 2. Transmission structure of TVC-EMA in one channel.

When the two actuators drive the load movements in the pitch and yaw directions (that is, the nozzle swing), there is coupling between their linear displacements. A previous study [7] derived mutual transformation functions between the linear displacement of the actuator and the desired rotation angle of the load (that is, the nozzle) using Euler angles, as shown in

$$T_{ib} = \begin{bmatrix} \cos q_1 \cos q_2 & -\sin q_1 & \cos q_1 \sin q_2 \\ \sin q_1 \cos q_2 & \cos q_1 & \sin q_1 \sin q_2 \\ -\sin q_2 & 0 & \cos q_2 \end{bmatrix} \tag{7}$$

$$\begin{cases} X_{2i} = T_{ib}X_{1i} \\ y_{ni} = \|X_{2i} - X_{0i}\| - \|X_{1i} - X_{0i}\| \quad (i = 1, 2) \end{cases} \tag{8}$$

where $X_{01} = [-290.0, -297.0, 0]^T$, $X_{02} = [-290.0, 0, -297.0]^T$, $X_{11} = [-852.3, -193.2, 0]^T$, $X_{12} = [-852.3, 0, -193.2]^T$, and the unit is millimeters.

III. PROPOSED CONTROL SCHEME

Considering the control of the two EMAs in the pitch and yaw directions, the double-channel control scheme is designed as Fig. 3. At the same time, because the feedback input (y_α) is the linear displacement of the actuator and it is desired that y_n track y_d, there is a compensation value ϵ_i for each channel [7]. In general, the command inputs are the pitch and yaw angles, so there are transformation functions that transfer the linear displacement of the actuator between the rotation angles in each channel.

In Fig. 3, EMA_1 and EMA_2 are the control laws of the pitch and yaw motions, respectively; F_1 and F_2 are the transformation functions; and f_1 and f_2 are compensation functions, which are presented as follows:

$$\varepsilon_{di} = k_i(y_{ai} - y_{ni}) \quad i = 1, 2 \tag{9}$$

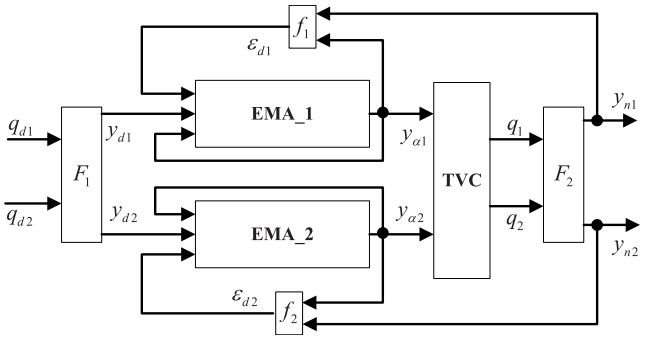

FIGURE 3. Control block diagram of TVC-EMA.

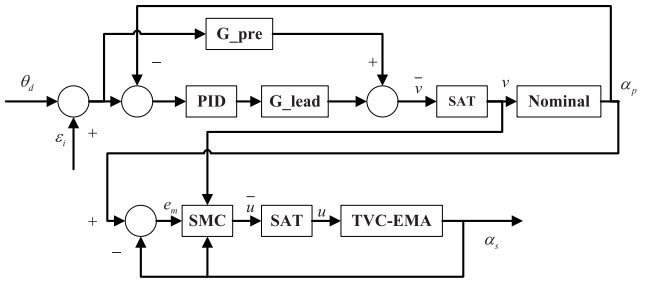

FIGURE 4. Control law block diagram of every channel.

As shown in Fig. 4, a compound control law composed of a PID controller and a sliding mode controller is proposed. According to Eq. (4), y_m could be transferred into the rotation angle of the motor α. The nominal model of TVC-EMA is controlled by a PID controller, and the TVC-EMA plant is controlled by SMC. A nominal model can be obtained by simplifying the transfer function using constant parameters so that the PID controller will not face parameter perturbation. When the TVC-EMA plant does generate parameter perturbation, the SMC will make up for the effect. The output of the nominal model (α_p) will track the command signal (θ_d), and it serves as the input of the SMC. Meanwhile, the output of the plant (α_s) will track α_p and the command signal. in Fig. 4, the SAT is a limiter that keeps the voltage amplitude within 54 V because of the limited power, and this is consistent with the actual situation of the aircraft engine.

In addition, if SMC is used alone, it will introduce the third derivative of the command signal, which makes the control voltage produce great chattering. The actual output of the control voltage does not reach the desired value of the SMC because of the voltage limiter, and the introduced compensation value, after the third-order differential, will increase the control voltage chattering.

From the control law block diagram, we see that the control performance is largely dependent on the control for the nominal model. Hence, feedforward compensation and advance compensation are added to improve the control performance of the PID controller, especially the position command tracking.

TABLE 1. Parameters of TVC-EMA.

Symbol	Value	Unit
R	2.2	Ω
L	8	mH
K_m	0.075	$V \cdot rad^{-1} \cdot s$
K_T	0.075	$N \cdot m \cdot A^{-1}$
B_a	0.001	$N \cdot m \cdot rad^{-1} \cdot s$
J_a	1.78×10^{-5}	$kg \cdot m^2$
i_g	3.0	
η_a	0.85	
B	6.0	mm
D	344.7	mm
K_l	2.0×10^8	$N \cdot m^{-1}$
B_n	55	$N \cdot m \cdot rad^{-1} \cdot s$
J_n	9.2	$kg \cdot m^2$
K_n	1.5×10^3	$N \cdot m \cdot rad^{-1}$

IV. PARAMETER DESIGN OF THE PROPOSED CONTROLLER

To evaluate the control scheme proposed by this paper and enable easy comparison with existing schemes, the parameter values of the TVC-EMA system model are the same as those used in a previous paper [7], as shown in Table 1. The input voltage limiters are omitted in the proposed controller parameter design process, and the controller with limiters is verified by the simulation.

A. NOMINAL MODEL BASED ON RESONANCE SUPPRESSION

The resonance causes the dynamic characteristics of the mechanical transmission parts to deteriorate. And the mechanical system will cause vibration at the frequency of the system resonance, resulting in damage to the mechanical equipment.

An open-loop transfer function $G(s)$ in which the input is the voltage U and the output is y_m will be obtained when the parameter values are input into the transfer function block diagram.

$$\begin{aligned} G(s) &= \frac{Y_m(s)}{U(s)} \\ &= \frac{167.65(s^2 + 5.978s + 2.583 \times 10^6)}{(s + 0.4175)(s^2 + 312.5s + 3.656 \times 10^4)} \\ &\quad \bullet \frac{1}{(s^2 + 24.28s + 3.935 \times 10^6)} \end{aligned} \tag{10}$$

Fig. 5 shows that there are two resonant points that are a notch resonance and a peak resonance in the high-frequency band, and their frequencies are 1607 rad/s and 1984 rad/s, respectively. To improve the anti-noise interference ability, they are offset using a peak filter and a notch filter, respectively [26]. Their transfer functions are as follows:

$$G_{peak\_filter} = \frac{s^2 + 2\xi_p \cdot 1607s + 2.583 \times 10^6}{s^2 + 5.978s + 2.583 \times 10^6} \tag{11}$$

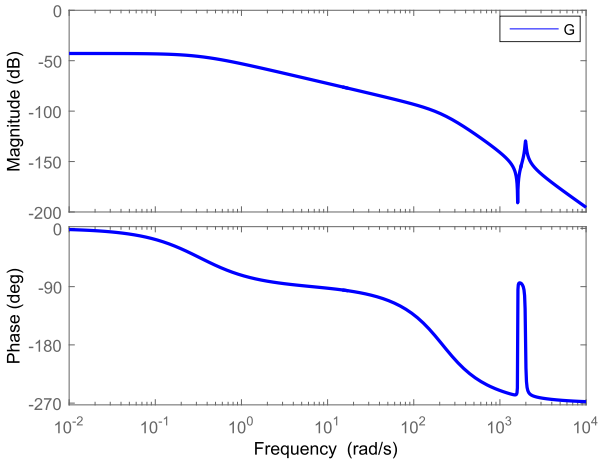

FIGURE 5. Open-loop Bode diagram of $G(s)$.

$$G_{notch\_filter} = \frac{s^2 + 24.28s + 3.935 \times 10^6}{s^2 + 2\xi_n \cdot 1984s + 3.935 \times 10^6} \quad (12)$$

where the damping coefficients are $\xi_p = 0.68$ and $\xi_n = 0.73$, respectively.

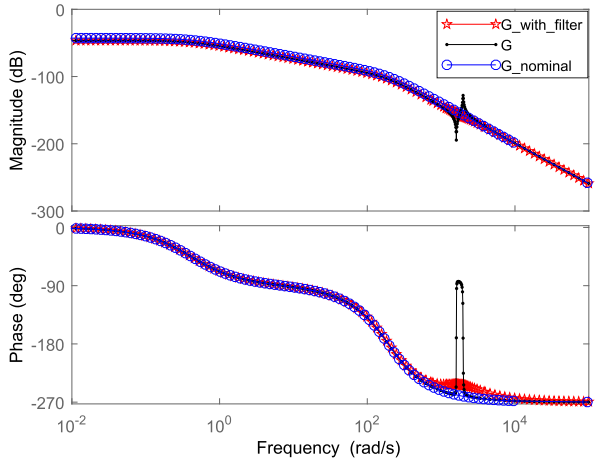

FIGURE 6. Bode diagrams of the TVC-EMA plant, the filter-corrected model and the fitted model.

G_{peak_filter}, G_{notch_filter} and G are connected in series to correct the TVC-EMA plant, and then, the nominal model of the TVC-EMA system is obtained by fitting the Bode diagram. Fig. 6 shows the Bode diagrams of the TVC-EMA plant, the filter-corrected model and the fitted model.

Upon fitting the Bode diagram, the nominal model of the TVC-EMA system is as follows:

$$G_{nominal} = \frac{110.1}{s^3 + 312.9s^2 + 3.669 \times 10^4 s + 1.526 \times 10^4} \quad (13)$$

B. PID CONTROLLER DESIGN

The closed-loop Bode diagrams of the plant and the nominal model are obtained by adding the same PID controller.

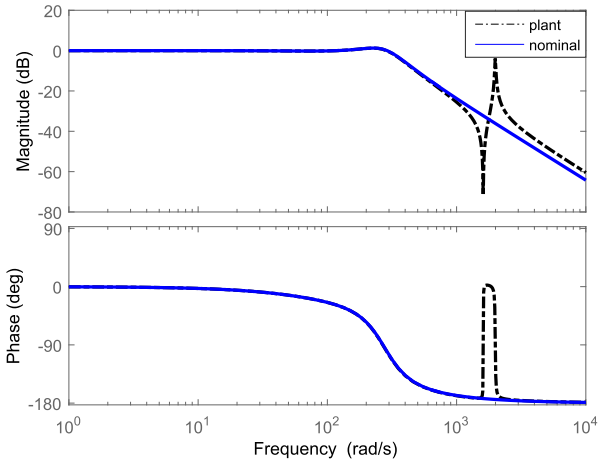

FIGURE 7. Closed-loop Bode diagrams of the plant and the nominal model.

Fig. 7 shows that the notch filter and the peak filter effectively suppress the high-frequency resonance of this TVC-EMA system.

In the proposed control scheme, the transfer function of the PID controller is designed as follows:

$$G_{PID} = 100500 + 6500\frac{1}{s} + 20s \quad (14)$$

and the transfer functions of the lead compensation and feed-forward compensation are as follows:

$$G_{lead} = \frac{s + 180}{s + 520} \quad (15)$$

$$G_{pre} = 350s \quad (16)$$

C. SMC DESIGN AND STABILITY ANALYSIS

According to the nominal model and considering that the linear displacement of the actuator is transferred to the angular displacement of the motor through Eq. (4), the dynamic model is

$$\dddot{\alpha}_p = -a_1\ddot{\alpha}_p - a_2\dot{\alpha}_p - a_3\alpha_p + b_1 v \quad (17)$$

where $a_1 = 312.9$, $a_2 = 3.669 \times 10^4$, $a_3 = 1.526 \times 10^4$, and $b_1 = 3.456 \times 10^5$.

According to Eq. (1)-Eq. (6), the actual dynamic model of the plant is

$$\dddot{\alpha}_s = -\widetilde{a}_1\ddot{\alpha}_s - \widetilde{a}_2\dot{\alpha}_s - \widetilde{b}_1\alpha_p - f + d \quad (18)$$

where $\widetilde{a}_1 = \frac{R+L}{L}$, $\widetilde{a}_2 = \frac{K_m K_T + RB_a}{LJ_a}$, $\widetilde{b}_1 = \frac{K_T}{LJ_a}$, $f = \frac{RT_L + L\dot{T}_L}{LJ_a}$, and d represents the interference and modeling uncertainty.

The tracking error of the SMC is defined as $e_m = \alpha_p - \alpha_s$, and the sliding surface is designed as

$$s = \sigma_1 e_m + \sigma_2 \dot{e}_m + \ddot{e}_m \quad (19)$$

where σ_1 and σ_2 meet the Hurwitz condition [27], that is, $\sigma_1 > 0$,$\sigma_2 > 0$.

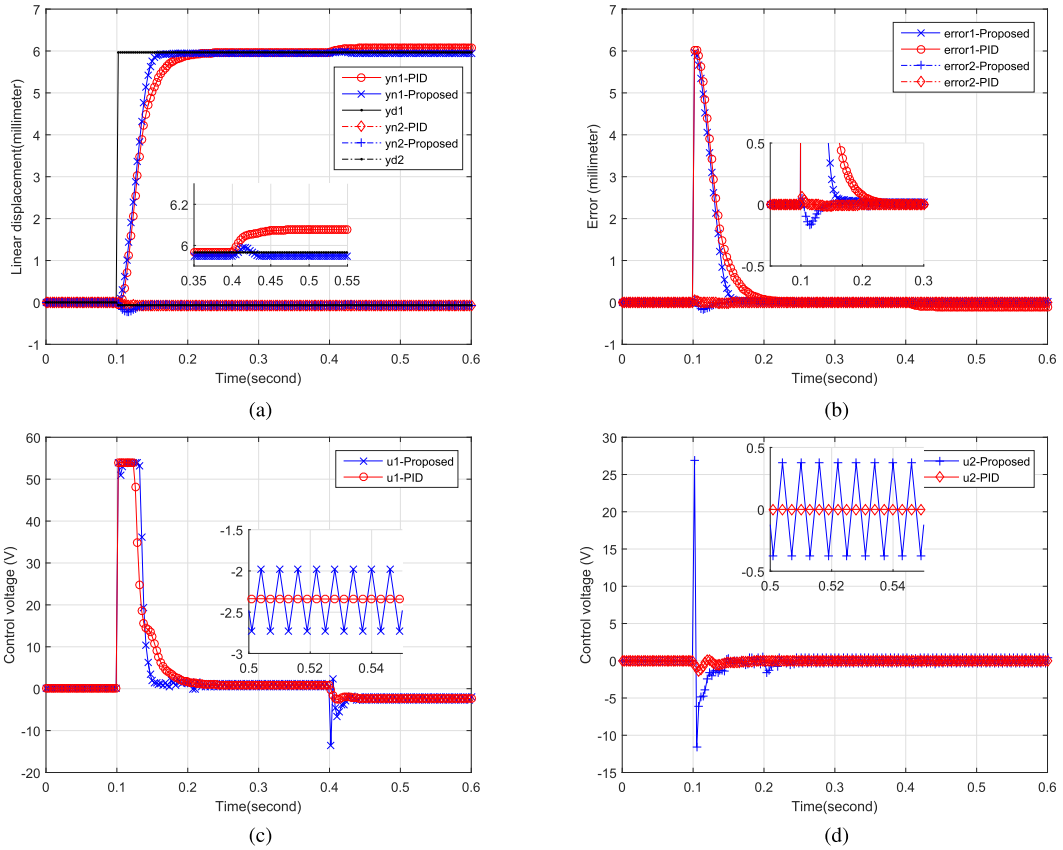

FIGURE 8. Step unit responses of the two actuators when $q_{d1} = 1°$, $q_{d2} = 0$: (a) linear displacement; (b) tracking error; (c) and (d) control voltage.

The sliding mode control law is designed as

$$u = \frac{1}{\widetilde{b}_1}(\sigma_1\dot{e}_m + \sigma_1\ddot{e}_m + \lambda_1 s + \lambda_2\,\mathrm{sgn}(s) + \widetilde{a}_1\ddot{\alpha}_s + \widetilde{a}_2\dot{\alpha}_s + \widetilde{b}_1\alpha_p + f + \ddot{\alpha}_p - d) \quad (20)$$

The Lyapunov function is defined as

$$V = \frac{1}{2}s^2 \quad (21)$$

and then, its first derivative is

$$\begin{aligned}\dot{V} &= s(\sigma_1\dot{e}_m + \sigma_1\ddot{e}_m + \dddot{\alpha}_p - \dddot{\alpha}_s)\\ &= s(\sigma_1\dot{e}_m + \sigma_1\ddot{e}_m + \dddot{\alpha}_p + \widetilde{a}_1\ddot{\alpha}_s + \widetilde{a}_2\dot{\alpha}_s \\ &\quad -\widetilde{b}_1 u - f + d)\end{aligned} \quad (22)$$

Taking the sliding mode control law into the first derivative of the Lyapunov function,

$$\dot{V} = -\lambda_1 \cdot s^2 - \lambda_2 \cdot |s| + d \cdot s \quad (23)$$

As long as $\lambda_1 > 0$ and $\lambda_2 > |d| > 0$, $\dot{V} \leq 0$ is feasible. This could be guaranteed by when $t \to \infty$, $e_m = 0$.

One of the premises necessary for the whole system to be stable is that the nominal model and PID controller system is stable. Its parameters must be selected so that the closed-loop poles are the s negative plane. To further reduce the chattering, the switch function $sgn(s)$ is replaced by the saturation function $sat(s)$, and Δ represents thickness of boundary layer and is set to 0.2.

$$sat(s) = \begin{cases} 1 & s > \Delta \\ \frac{s}{\Delta} & |s| \leq \Delta \\ -1 & s < \Delta \end{cases} \quad (24)$$

V. VERIFICATION

To evaluate the proposed control scheme, this paper uses a mixed PID controller composed of a PID controller and the bang-bang control introduced by reference [3] as the contrast method, and it is called the PID controller for simplification. MATLAB/SIMULINK is used for the simulation, and the step time is 0.003 seconds. In the case of satisfying the parameter limitation conditions and the control requirements, the parameters of SMC are set as follows: $\sigma_1 = 4 \times 10^4$ $\sigma_2 = 200$, $\lambda_1 = 180$, $\lambda_2 = 10^5$, $k_1 = 1$, and $k_2 = 1$.

A. UNIT STEP RESPONSE AND DISTURBANCE STEP RESPONSE

Because the control law schemes for the pitch and yaw directions are the same, this paper just simulates the unit step response in the pitch channel. At the initial time, all the inputs, including the pitch angle, the yaw angle and the disturbance torque, are 0. Then, at 0.1 seconds, the pitch angle is given

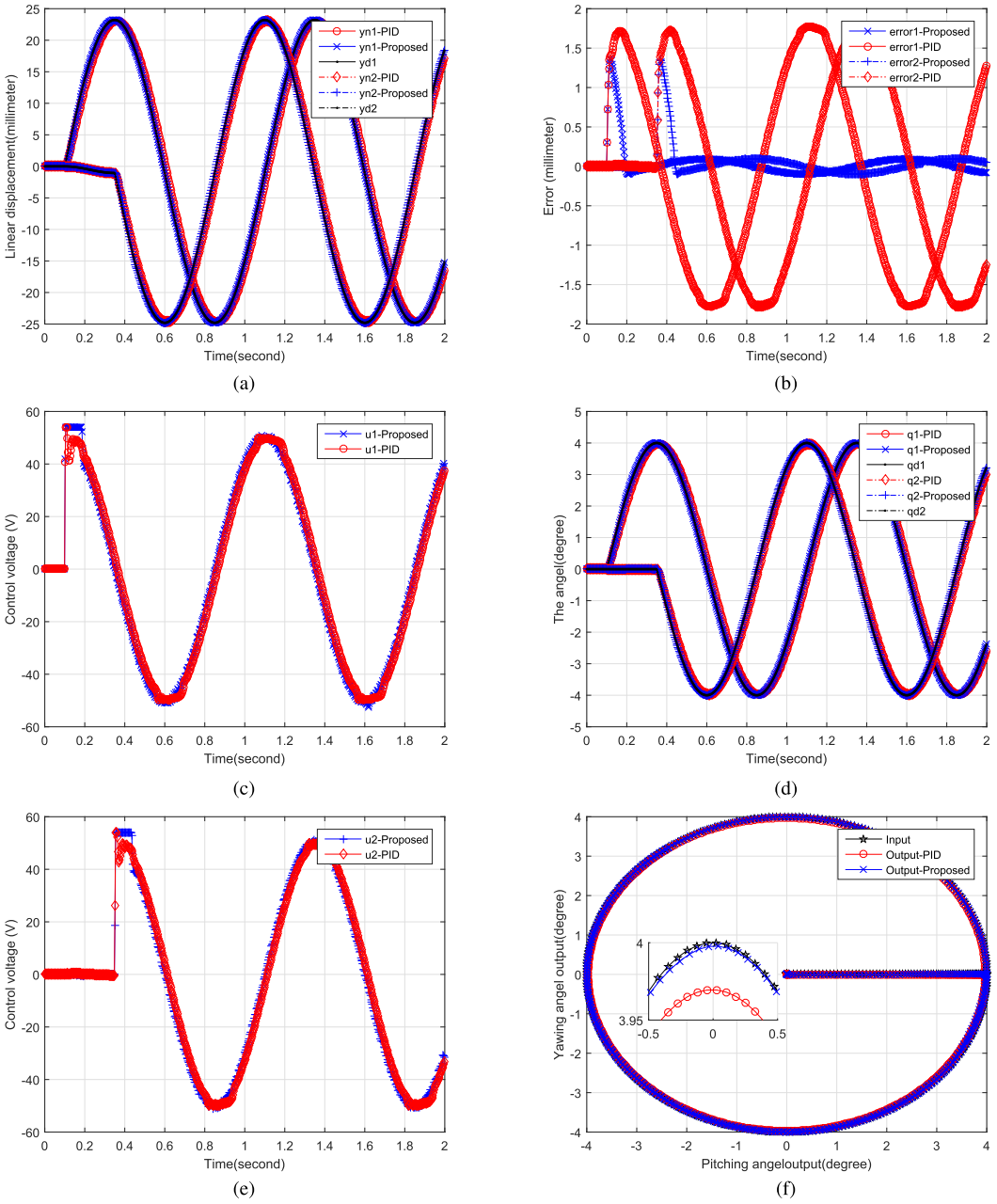

FIGURE 9. Position tracking response of TVC-EMA: (a) linear displacement of the actuator; (b) tracking error; (c) and (d) control voltage; (e) swing angle of the nozzle; (f) movement of the nozzle.

a unit step signal. After the unit step response is stabilized, at 0.4 seconds, a torque disturbance signal T_d is provided to the pitch channel. The response curves are shown in Fig. 9, and the equation of the error is as follows:

$$error_i = y_{di} - y_{ni} \quad (i = 1, 2) \tag{25}$$

The nozzle movement is a combination of pitch and yaw motions. Although the yaw command input is 0, there is a slight step in the actuator of the yaw channel. The results show that there is no overshoot and that the steady-state error is less than 0.2% under the two different control law schemes. When using the PID control law and the proposed control law based on SMC, settling times are 0.102 seconds and 0.082 seconds, respectively. The magnification in Fig. 8(a) shows that the ability of this compound control law to resist a load torque disturbance is much stronger than that of a PID controller. The magnification of Fig. 8(b) shows that this compound control law has a slight overshoot, but the duration is very short, less than 0.04 seconds. Additionally, the absolute value of the overshoot is small, so its effect is negligible. Fig. 8(c) and Fig. 8(d) show that there is slight chatter in the control voltage of this compound control law. In the 0.4 seconds, the partial enlarged detail of Fig. 8(a) shows that the proposed control scheme can suppress

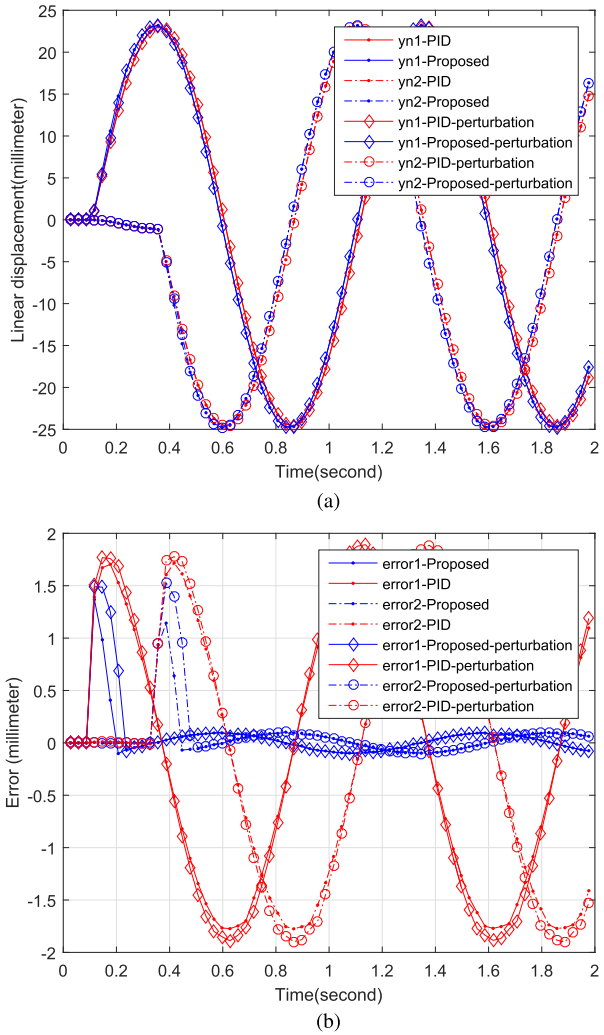

FIGURE 10. Position tracking response under parameter disturbances: a) linear displacement of the actuator; b) tracking error.

interference torque well, but the PID controller cannot. When T_d is added and using the proposed control scheme, y_n deviates from the desired value but returns to the desired value after 0.05 seconds, and the maximum error is less than 0.04 millimeters. Meanwhile, when using the PID controller, the errors are greater, and they slowly decrease over more than 20 seconds. The enlarged details of Fig. 8(c) and Fig. 8(d) show that the chattering of the control voltage is less than 1 V.

B. POSITION TRACKING

The most important performance target of TVC-EMA is the position command tracking. The input of the disturbance torque is set to 0, and this value is maintained. The sine and cosine command signals, that the amplitude is 4° and the frequency is 1 Hz, respectively, are sent to the pitch channel and yaw channel. The command signal of the yaw lags behind that of the pitch channel by 0.25 seconds, that is, a quarter cycle. The simulation results are presented in Fig. 9. Fig. 9(b) shows that this compound control law produces a large error at the initial time, but it decreases within 0.1 seconds and thereafter remains below 0.1 mm. The tracking error of the PID controller is greater than that of this compound control law, with a maximum absolute value greater than 1.6 mm. Fig. 9(c) and Fig. 9(d) show the control voltage curves of the two channels. Fig. 10(e) shows the load movement following a circular motion, and its magnification shows that the output load track of the compound control law is closer to the command track than for the PID controller. Taken together, the position tracking performance of the compound control law based on SMC is better than that of the PID controller, and the chattering of the control voltage is slight.

C. ROBUSTNESS TO THE MODEL PARAMETER UNCERTAINTY

To perform a robustness analysis on the proposed control method, both B_a and J_n are set to a step of 30%, and the command signals are the same as those in the position tracking simulation. Fig. 10 shows that the position tracking errors undergo changes only in the initial 0.1 seconds, and thereafter, the errors are almost the same as those in the situation before the parameter disturbances. However, the position tracking errors of the PID controller have strikingly changed, and the maximum values are greater than 0.1 mm. Thus, we can determine that when there is modeling error and parameter uncertainty, the robustness of this compound control law based on SMC is better than that of the PID controller.

VI. CONCLUSION

This paper introduces the TVC-EMA system in which one nozzle is driven by two actuators, and a nominal model for the TVC-EMA system based on resonance suppression is obtained. A compound control law composed of a PID controller and a sliding mode controller is proposed, and the stability proof of this SMC is provided in the sense of the Lyapunov method. It overcomes the shortcoming of poor robustness of the pure PID controller, and the chatter of the control signal produced by the SMC is slight. Simulations based on MATLAB manifest that this compound control law has a fast dynamic property and stronger robustness and better position tracking performance than the PID controller.

REFERENCES

[1] F.-K. Yeh, "Adaptive-sliding-mode guidance law design for missiles with thrust vector control and divert control system," *IET Control Theory Appl.*, vol. 6, no. 4, pp. 552–559, 2012.
[2] A. Steer, "Integrated control of a second generation supersonic commercial transport aircraft using thrust vectoring," in *Proc. Guidance, Navigat., Control Co-Located Conf.*, 2000, p. 454.
[3] P. H. Zipfel, *Modeling and Simulation of Aerospace Vehicle Dynamics*. Washington, DC, USA: AIAA, 2003.
[4] D. V. Lazić and M. R. Ristanović, "Electrohydraulic thrust vector control of twin rocket engines with position feedback via angular transducers," *Control Eng. Pract.*, vol. 15, no. 5, pp. 583–594, 2007.
[5] S. Jianguo, V. Vasilyev, and B. Ilyasov, *Advanced Multivariable Control Systems of Aeroengines*. Beijing, China: Astronautics Press, 2005.
[6] D. E. Schinstock and T. A. Haskew, "Identification of continuous-time, linear, and nonlinear models of an electromechanical actuator," *J. Propuls. Power*, vol. 13, no. 5, pp. 683–690, 1997.

[7] Y. Li, H. Lu, S. Tian, Z. Jiao, and J.-T. Chen, "Posture control of electromechanical-actuator-based thrust vector system for aircraft engine," *IEEE Trans. Ind. Electron.*, vol. 59, no. 9, pp. 3561–3571, Sep. 2012.
[8] D. E. Schinstock, D. A. Scott, and T. A. Haskew, "Transient force reduction in electromechanical actuators for thrust-vector control," *J. Propuls. Power*, vol. 17, no. 1, pp. 65–72, 2001.
[9] A. Kayran and M. O. Nalci, "Aeroservoelastic modeling and analysis of a missile control surface with a nonlinear electromechanical actuator," in *Proc. AIAA Atmos. Flight Mech. Conf.*, 2013, pp. 2014–2055.
[10] V. Utkin, "Variable structure systems with sliding modes," *IEEE Trans. Autom. Control*, vol. AC-22, no. 2, pp. 212–222, Apr. 1977.
[11] J. Y. Hung, W. Gao, and J. C. Hung, "Variable structure control: A survey," *IEEE Trans. Ind. Electron.*, vol. 40, no. 1, pp. 2–22, Feb. 1993.
[12] W. Gao and J. C. Hung, "Variable structure control of nonlinear systems: A new approach," *IEEE Trans. Ind. Electron.*, vol. 40, no. 1, pp. 45–55, Feb. 1993.
[13] J. Fei and H. Ding, "Adaptive sliding mode control of dynamic system using RBF neural network," *Nonlinear Dyn.*, vol. 70, no. 2, pp. 1563–1573, Oct. 2012.
[14] J. Fei and C. Lu, "Adaptive sliding mode control of dynamic systems using double loop recurrent neural network structure," *IEEE Trans. Neural Netw. Learn. Syst.*, to be published.
[15] J. H. Wiest and G. D. Buckner, "Indirect intelligent sliding mode control of antagonistic shape memory alloy actuators using hysteretic recurrent neural networks," *IEEE Trans. Control Syst. Technol.*, vol. 22, no. 3, pp. 921–929, May 2014.
[16] R.-J. Wai, K.-L. Chuang, and J.-D. Lee, "On-line supervisory control design for maglev transportation system via total sliding-mode approach and particle swarm optimization," *IEEE Trans. Autom. Control*, vol. 55, no. 7, pp. 1544–1559, Jul. 2010.
[17] I. Eker, "Sliding mode control with PID sliding surface and experimental application to an electromechanical plant," *ISA Trans.*, vol. 45, no. 1, pp. 109–118, 2006.
[18] F. Cupertino, D. Naso, E. Mininno, and B. Turchiano, "Sliding-mode control with double boundary layer for robust compensation of payload mass and friction in linear motors," *IEEE Trans. Ind. Appl.*, vol. 45, no. 5, pp. 1688–1696, Sep./Oct. 2009.
[19] L. Jinkun, *Sliding Mode Control Design and MATLAB Simulation*. Beijing, China: Tsinghua Univ. Press, 2012.
[20] I. Eker, "Second-order sliding mode control with PI sliding surface and experimental application to an electromechanical plant," *Arabian J. Sci. Eng.*, vol. 45, no. 7, pp. 1969–1986, 2012.
[21] H. Lu, Y. Li, and C. Zhu, "Robust synthesized control of electromechanical actuator for thrust vector system in spacecraft," *Comput. Math. Appl.*, vol. 64, no. 5, pp. 699–708, 2012.
[22] N. Wang, W. Lin, and J. Yu, "Sliding-mode-based robust controller design for one channel in thrust vector system with electromechanical actuators," *J. Franklin Inst.*, 2016. [Online]. Available: http://www.sciencedirect.com/science/article/pii/S0016003216303325
[23] H. K. Sang and M.-J. Tahk, "Modeling and experimental study on the dynamic stiffness of an electromechanical actuator," *J. Spacecraft Rockets*, vol. 53, no. 4, pp. 708–719, 2016.
[24] D. E. Schinstock, D. A. Scott, and T. A. Haskew, "Modeling and estimation for electromechanical thrust vector control of rocket engines," *J. Propuls. Power*, vol. 14, no. 4, pp. 440–446, 1998.
[25] R. Salloum, M. R. Arvan, and B. Moaveni, "Identification, uncertainty modelling, and robust controller design for an electromechanical actuator," in *Proc. Int. Conf. Control, Autom., Robot. Embedded Syst.*, 2013, pp. 1–6.
[26] M. Yang, L. Hao, and D. Xu, "Online suppression of mechanical resonance based on adapting notch filter," *J. Harbin Inst. Technol.*, vol. 46, no. 4, pp. 63–69, 2014.
[27] S. Bai, P. Ben-Tzvi, Q. Zhou, and X. Huang, "Variable structure controller design for linear systems with bounded inputs," *Int. J. Control, Autom. Syst.*, vol. 9, no. 2, p. 228, 2011.

BING YU received the B.S. degree in automation, and the M.S. and Ph.D. degrees in navigation guidance and control from Southeast University, China, in 2002, 2009, and 2009, respectively. His current research interests include the control and testing of aircraft engines.

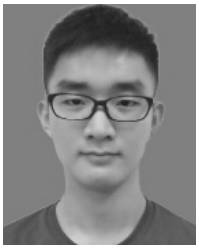

WENJUN SHU received the B.S. degree in flight vehicle propulsion engineering from the Nanjing University of Aeronautics and Astronautics, China, in 2016. He is currently pursuing the master's degree in power machinery and engineering with the Nanjing University of Aeronautics and Astronautics.